frontiers in Marine Science

ORIGINAL RESEARCH
published: 20 January 2022
doi: 10.3389/fmars.2021.775653

Planktonic Tintinnid Community Structure Variations in Different Water Masses of the Arctic Basin

Chaofeng Wang[1,2,3], Xiaoyu Wang[4], Zhiqiang Xu[2,5], Qiang Hao[6], Yuan Zhao[1,2,3], Wuchang Zhang[1,2,3]* and Tian Xiao[1,2,3]*

[1] CAS Key Laboratory of Marine Ecology and Environmental Sciences, Institute of Oceanology, Chinese Academy of Sciences, Qingdao, China, [2] Laboratory for Marine Ecology and Environmental Science, Qingdao National Laboratory for Marine Science and Technology, Qingdao, China, [3] Center for Ocean Mega-Science, Chinese Academy of Sciences, Qingdao, China, [4] Frontiers Science Center for Deep Ocean Multispheres and Earth System, Key Laboratory of Physical Oceanography, Ocean University of China, Qingdao, China, [5] Jiaozhou Bay Marine Ecosystem Research Station, Institute of Oceanology, Chinese Academy of Sciences, Qingdao, China, [6] Key Laboratory of Marine Ecosystem Dynamics, Second Institute of Oceanography, Ministry of Natural Resources, Hangzhou, China

OPEN ACCESS

Edited by:
Martin Edwards,
Plymouth Marine Laboratory,
United Kingdom

Reviewed by:
Weiwei Liu,
South China Sea Institute of Oceanology, Chinese Academy of Sciences (CAS), China
Henglong Xu,
Ocean University of China, China
S. Sai Elangovan,
National Institute of Oceanography, Council of Scientific and Industrial Research (CSIR), India

***Correspondence:**
Yuan Zhao
yuanzhao@qdio.ac.cn
Wuchang Zhang
wuchangzhang@qdio.ac.cn

Specialty section:
This article was submitted to Marine Ecosystem Ecology, a section of the journal Frontiers in Marine Science

Received: 15 September 2021
Accepted: 21 December 2021
Published: 20 January 2022

Citation:
Wang C, Wang X, Xu Z, Hao Q, Zhao Y, Zhang W and Xiao T (2022) Planktonic Tintinnid Community Structure Variations in Different Water Masses of the Arctic Basin. Front. Mar. Sci. 8:775653. doi: 10.3389/fmars.2021.775653

Information on tintinnid community structure variations in different water masses in the Arctic Basin is scarce. During the summer of 2020, tintinnid diversity and vertical distribution were investigated in the Arctic Ocean. A total of 21 tintinnid species were found in five water masses and each water mass had a unique tintinnid community structure. In the Pacific Summer Water (PSW), *Salpingella* sp.1 occupied the top abundance proportion (61.8%) and originated from the North Pacific. In the Remnant Winter Water (RWW), *Acanthostomella norvegica* occupied the top abundance proportion (85.9%) and decreased northward. In the Mixed Layer Water, Pacific Winter Water, and Atlantic-origin Water, *Ptychocylis urnula* had the highest abundance proportion (67.1, 54.9, and 52.2%, respectively). The high abundance distribution area of *Salpingella* sp.1 and *A. norvegica* were separated by the boundary of the Beaufort Gyre and Transpolar Drift. The above species could be indicator species of each water masses. The highest abundance proportion of *Salpingella* sp.1 contributes 81.9% to the dominance of 12–16 μm lorica oral diameter in the PSW, which indicated that the preferred food items of tintinnid were also getting smaller. The occurrence of North Pacific tintinnid in the PSW might be due to the increasing Pacific Inflow Water. Further studies are needed to explore the lasting period of this species and whether it can establish a local population under rapid Arctic warming progress.

Keywords: Arctic Ocean, tintinnid, community structure, water mass, variation, indicator species

INTRODUCTION

The Arctic Ocean is one of the most sensitive regions to global warming (Trenberth et al., 2007) and contains a complex of water masses (Gerdes and Schauer, 1997). Between the Mendeleev Ridge and Canada Basin, different currents from the Atlantic Ocean, Arctic shelves, and the Pacific Ocean converge during summer (McLaughlin et al., 2004; Aksenov et al., 2011; Bluhm et al., 2015). Each water mass has unique hydrographic features and zooplankton communities, e.g., tintinnids can

act as indicator species of different water masses in the North Pacific (Kato and Taniguchi, 1993); gelatinous zooplankton can act as an indicator of atlantification in the North Atlantic (Mańko et al., 2020); and the tintinnid community structures vary in different water masses in the Southern Ocean (Liang et al., 2018, 2019). As for tintinnids, an important component of microzooplankton, they are widely distributed in the Arctic Ocean (e.g., Dolan et al., 2014, 2017; Wang et al., 2019).

Tintinnids (Ciliophora: Spirotrichea: Choreotrichia) are planktonic ciliates with loricae around their body (Lynn, 2008). They are primary consumers of pico-(0.2–2 μm) and nano-(2–20 μm) sized plankton, as well as important food sources for metazoans and fish larvae (Stoecker et al., 1987; Dolan et al., 1999; Gómez, 2007). Tintinnid play an important role in material circulation and energy flow from the microbial food web into the traditional food chain (Azam et al., 1983; Pierce and Turner, 1992; Calbet and Saiz, 2005). Due to their high frequencies, identifiable morphology, and outer lorica protection, tintinnid species have been suggested as favorable bioindicators of various oceanographic conditions (Kato and Taniguchi, 1993; Rakshit et al., 2017). Previous studies have exhibited the species list of the Arctic Ocean (Dolan et al., 2017). However, to date, no data exist relating to tintinnid community structure variations in the different water masses of the Arctic Basin.

The Arctic Ocean is experiencing an increase in Pacific Inflow Water because of global warming (Woodgate, 2018), which has changed local hydrographic features (Møller and Nielsen, 2020; Polyakov et al., 2020). Pacific plankton species are transported further north into the Arctic Ocean with increasing inflows (Grebmeier and Harvey, 2005; Hopcroft et al., 2010). Studies on the northward transportation of Arctic Ocean plankton have mainly focused on phytoplankton and mesozooplankton communities (Ershova et al., 2015; Wassmann et al., 2015; Hunt et al., 2016; Wang et al., 2018; Lewis et al., 2020; Wang Y. et al., 2020; Zhuang et al., 2021). Ershova et al. (2015) found that Pacific copepod (*Eucalanus bungii*, *Metridia pacifica,* and *Neocalanus* spp.) distributions had extended about five degrees further north than in 1946 in the Chukchi Sea. However, there was no similar report for tintinnids.

In the Pacific Gateway, the Pacific Inflow Water transports Pacific tintinnids into the Chukchi Sea, mixing them with the Arctic tintinnid community (Li et al., 2016; Wang et al., 2019). Pacific water would descend in subsurface layers of the Canada Basin, forming the Pacific Summer Water (PSW) (Steele et al., 2004). Pacific tintinnids were not found in the PSW in previous investigations (Dolan et al., 2014; Li et al., 2016; Wang et al., 2019). However, with the increase of Pacific Inflow Water (Woodgate, 2018) the Pacific tintinnids might be transported in the PSW of the Canada Basin.

This paper studied the tintinnid community in the Arctic Basin. We hypothesized that the tintinnid community in different water masses of the Arctic Ocean is different. Another aim of this study was to examine whether Pacific tintinnids were transported into the PSW of the Canada Basin, which serves as baseline data for monitoring changes in the planktonic zooplankton community due to increasing Pacific Inflow and global warming in the Arctic Ocean.

MATERIALS AND METHODS

Samples were collected between 29 July and 30 August 2020, during the 11th Chinese National Arctic Research Expedition aboard R.V. "Xuelong 2." Ice cover data were sourced from Sea Ice Remote Sensing at the University of Bremen[1]. Water samples were collected at 43 stations (**Supplementary Table 1**) along five transects (Tr.): Tr. R (Sts. 1–9), P1 (Sts. 1–5, R2, 6–8), P2 (Sts. 1–3, R4, 4–10), and P3 (Sts. 1–6, R6, 7–13), E (Sts. 1, 2, P1-2, P2-1, 3, P3-4) (**Figure 1** and **Supplementary Table 1**). All stations (except R1, 196 m) were deeper than 200 m (**Supplementary Table 1**).

At each station, vertical profiles of temperature and salinity were obtained from the surface (3 m) to 200 m (except St. R1, where the bottom sample was from 189 m) using an SBE911-conductivity-temperature-depth (CTD) unit. Water masses were identified by referring to Morison et al. (1998); Steele et al. (2004), Timmermans et al. (2014), and Gong and Pickart (2016).

Water samples were taken from 3 (surface), 25, 50, 75, 100, 150, and 200 m at most stations using 12 L Niskin bottles attached to a CTD rosette wheel. Each sampling depth was regarded as one sampling point. The sampling depths were adapted to DCM (deep Chl *a* maximum) layer if it was within 10 m of any nearby sampling depth. Chlorophyll *a* (Chl *a*) concentration was determined by filtering 500 mL of seawater through a Whatman GF/F glass fiber filter. Plankton retained on the filter was extracted in 90% (vv^{-1}) acetone. Fluorescence was measured according to the JGOFS protocol (Knap et al., 1996) using a Turner Trilogy fluorometer Model 10.

A total of 301 water samples (1 L) were collected for tintinnid analysis. Samples were fixed with acid Lugol's (1% final concentration) and stored in darkness at 4°C during the cruise. In the laboratory, water samples were concentrated to about 200 mL by siphoning off the supernatant after settling the sample for 60 h. This settling and siphoning process was repeated until a final concentrated volume of 50 mL was achieved, which was then settled in two Utermöhl counting chambers (25 mL per chamber) (Utermöhl, 1958) for at least 24 h. Tintinnids were counted using an Olympus IX 73 inverted microscope (100× or 400×) according to the process of Lund et al. (1958) and Utermöhl (1958).

During the counting process, the sizes of at least 10 loricae of each species were measured. Tintinnid taxa were identified according to the size and shape of the loricae following Taniguchi (1976), Davis (1977, 1981), Zhang et al. (2012), Dolan et al. (2014, 2017), Li et al. (2016), and Wang et al. (2019). Because mechanical and chemical disturbance during collection and fixation can detach the tintinnid protoplasm from the loricae (Paranjape and Gold, 1982; Alder, 1999), we included empty tintinnid loricae in cell counts. Empty loricae and loricae with plasma for species with comparatively high abundance were counted separately.

Biogeographically, tintinnid genera were classified as oceanic and neritic (Pierce and Turner, 1993; Dolan and Pierce, 2013). Lorica oral diameter (LOD) was divided into size classes in 4 μm increments (12–16 μm, 16–20 μm, etc.) following Dolan et al. (2016). Occurrence frequency (OF,%) was calculated by dividing

[1]https://seaice.uni-bremen.de/sea-ice-concentration/

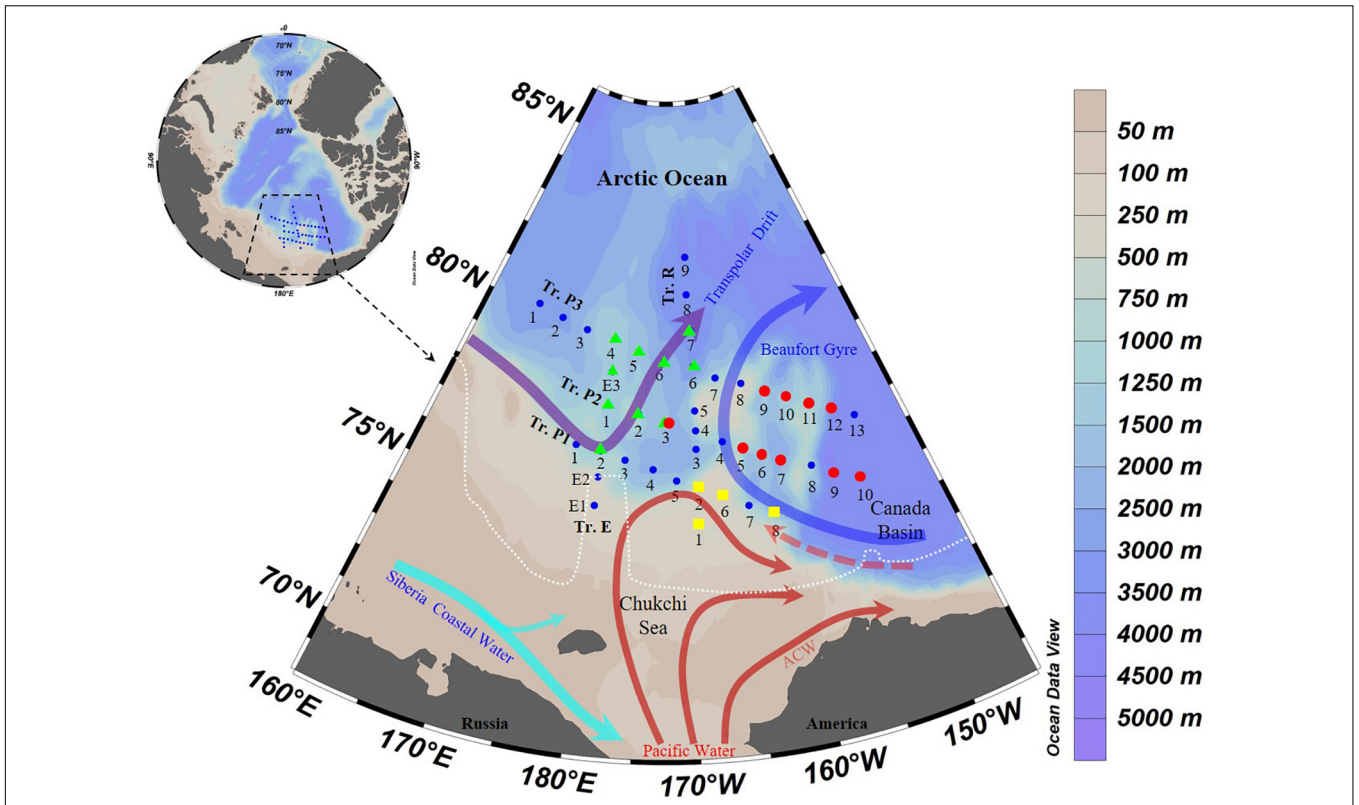

FIGURE 1 | Transects (Tr.) and survey stations in the Arctic Ocean. White dotted line delimits the ice edge, where covered by sea ice in the Arctic Ocean on 1 August 2020 [Sea Ice Remote Sensing, University of Bremen (https://nsidc.org/data/seaice_index)]; Arrows showed currents following Aksenov et al. (2016), Hunt et al. (2016), Li et al. (2019), and Zhong et al. (2019); ACW, Alaskan Coastal Water. Red circles, stations of *Salpingella* sp.1 occurred in high abundance (≥30 ind. L^{-1}); Green triangle, stations of *Acanthostomella norvegica* occurred in high abundance; Yellow square, stations where neritic species occurred.

all sampling points in one water mass by the number of sampling points where one species occurred. Abundance proportion (%) was calculated by dividing the total average abundance of all tintinnids with the average abundance of one species in one water mass. We used the Shannon index (H') (Shannon, 1948) and Simpson index (λ) (Simpson, 1949) to test tintinnid diversity indices in different water masses.

RESULTS

Hydrographic Features

Most stations were covered by sea ice on 1 August (**Figure 1**). Two high temperature ($>-0.5°C$) areas were present: between 25–100 and 150–200 m (**Figure 2**). The high temperature area at 25–100 m depths appeared only in the eastern part of transects P1, P2, and P3. Salinity was low in the surface layers (27.7 ± 0.8), then increased to 200 m depth (34.2 ± 0.6) (**Figure 2**). The deep Chl *a* maximum (DCM) layers occurred between 25 and 75 m, and the highest Chl *a* concentration (2.68 $\mu g\ L^{-1}$) occurred on the Chukchi Sea shelf (38 m of St. R2) (**Figure 2**).

Vertically, five water masses were identified according to hydrographic features: Mixed Layer Water (MLW), Remnant Winter Water (RWW), Pacific Summer Water (PSW), Pacific Winter Water (PWW), and Atlantic-origin Water (AtW) (**Figure 2** and **Table 1**). The MLW was characterized by low temperature ($<-0.5°C$) and salinity (26.5–29.0) and occurred mainly in the upper 20 m of most stations (except St. R4 and P3-7, where occurred from surface to 25 m). Transect R divided the three P transects into two parts according to the position of the rest of the four water masses. The RWW and AtW occurred in western parts of transects P1, P2, and P3, and the PSW and PWW occurred mainly in the eastern parts of these transects (**Figure 2**).

Tintinnid Species Composition

A total of 21 tintinnid species belonging to 7 genera were identified, and there were 7, 7, 8, 9, and 17 species in the PSW, RWW, MLW, PWW, and AtW, respectively (**Table 2**). According to their average abundance (AA) and occurrence frequency (OF), all tintinnid species were classified into abundant ($AA \geq 3.0$ ind. L^{-1} and $OF \geq 20\%$) and rare species (rest) (**Table 2**). Among the nine species in oceanic genera, *Salpingella* sp. 1, *Acanthostomella norvegica,* and *Ptychocylis urnula* (**Supplementary Figure 1**) were abundant species (**Table 2**). Empty loricae occupied 1.3, 29.3, and 41.0% in all loricae for the three abundant species, respectively.

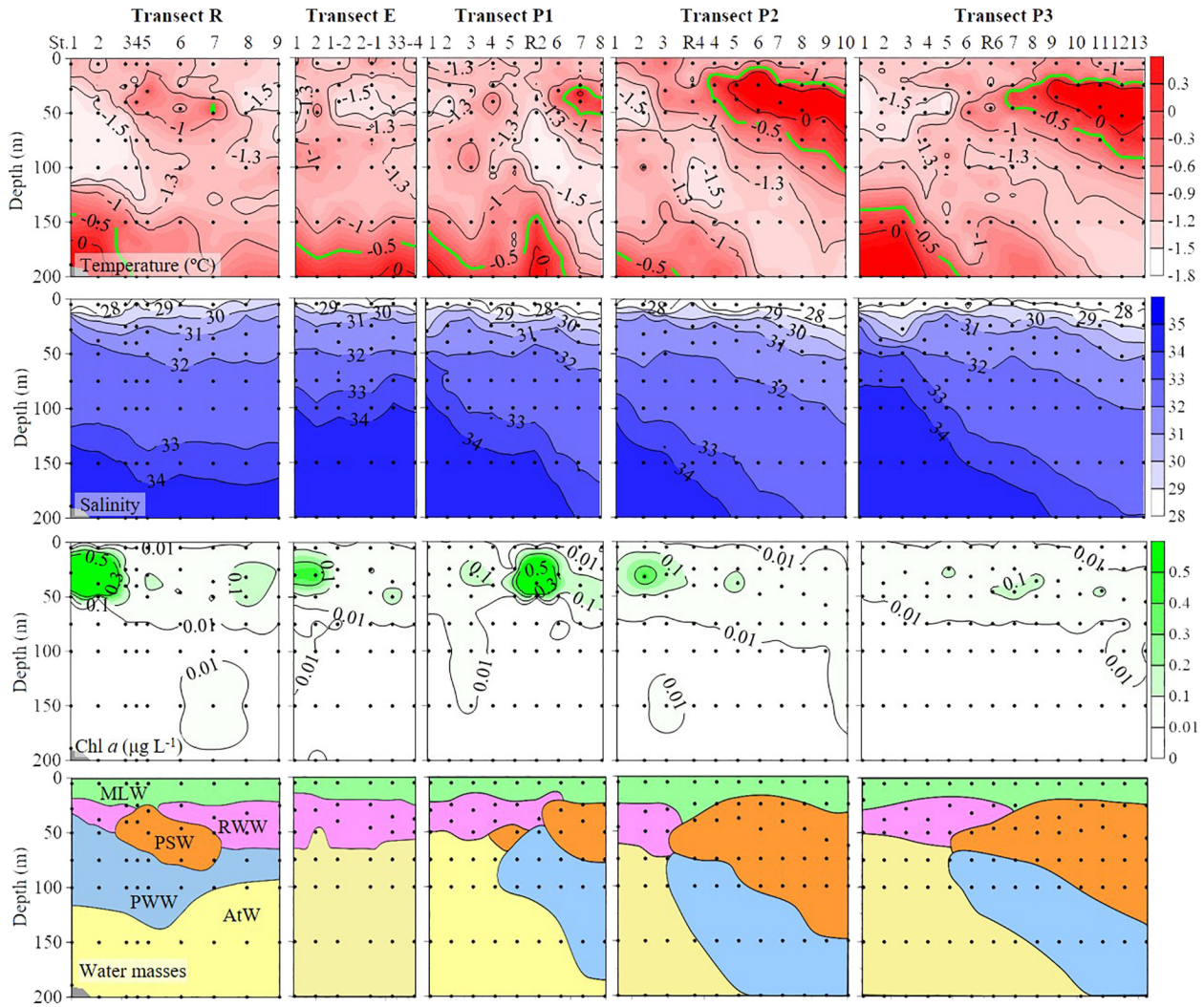

FIGURE 2 | Temperature, salinity, Chlorophyll *a* (Chl *a*), and different water mass profiles from the surface to 200 m (or bottom). Black dots, sampling points; PSW, Pacific Summer Water; PWW, Pacific Winter Water; RWW, Remnant Winter Water; MLW, Mixed Layer Water; AtW, Atlantic-origin Water.

TABLE 1 | Water mass classification according to hydrographic features in the study area.

Water mass	Temperature (°C)	Salinity	Depth (m)
Mixed Layer Water (MLW)	<−0.5	26.5–29.0	0–25
Remnant Winter Water (RWW)	<−1.0	30.0–32.0	25–65
Pacific Summer Water (PSW)	(−1.0)–1.0	29.0–32.5	20–120
Pacific Winter Water (PWW)	<−1.3	32.0–33.2	100–200
Atlantic-origin Water (AtW)	(−1.8)–1.0	32.5–34.9	70–200

Twelve species of neritic genera (*Leprotintinnus*, *Stenosemella,* and *Tintinnopsis*) occurred with low abundance only at 4 stations near the Chukchi shelf (**Figure 1**). Their total abundance reached 28 ind. L^{-1} at 28 m depth in the shallowest station St. R1. In other stations (Sts. R2, P1-6, P1-8), their total abundance was lower than 2 ind. L^{-1}. These species occurred only in the MLW, PWW, and AtW (**Table 2**).

Total Tintinnid Abundance in Each Water Mass

Total tintinnid abundance ranged from 0 to 454 ind. L^{-1} and high abundance (≥30 ind. L^{-1}) distributed in upper 100 m layers (**Figure 3**). As for different water masses, the RWW (80.5 ± 102.3 ind. L^{-1}) had the highest average total tintinnid abundance, followed by the PSW (36.0 ± 58.8 ind. L^{-1}). The other three water masses had a low average abundance: 2.1 ± 2.3, 5.7 ± 7.3, and 3.5 ± 5.7 ind. L^{-1} in the PWW, MLW, and AtW, respectively (**Figure 4**).

Discrete distribution of high tintinnid abundance characterized the eastern and western parts of the study area (**Figure 3**). The transect R represents a boundary for these two high abundance parts. In transects P1, P2, and P3, eastern and western high abundance parts overlapped with the PSW and RWW, respectively (**Figures 2**, **3**). Along with the transect R, tintinnid abundance first decreased northward to St. R5, then

TABLE 2 | Tintinnid species average abundance (AA, ind. L^{-1}) and occurrence frequency (OF, %) in different water masses of the Arctic Ocean.

Species	LOD (n = 10)	LL (n = 10)	PSW		PWW		RWW		MLW		AtW		Total waters	
			AA	OF	AA	OF	AA	OF	AA	OF	AA	OF	AA	OF
Oceanic species														
Acanthostomella norvegica	26.9 ± 1.0	39.8 ± 3.6	2.8 ± 4.6	50.0	0.1 ± 0.3	13.6	69.2 ± 99.9	66.7	1.4 ± 3.4	32.7	0.8 ± 1.5	36.3	8.6 ± 39.1	37.9
*Coxliella ampla**	58.5 ± 1.3	74.9 ± 2.7	0.0 ± 0.3	2.0	–	–	0.0 ± 0.2	3.0	–	–	0.0 ± 0.1	0.8	0.0 ± 0.1	1.0
*C. cymatiocoides**	70.7	154.2	–	–	–	–	–	–	0.0 ± 0.1	2.0	–	–	0.0 ± 0.1	0.3
Ptychocylis acuta	67.7 ± 3.6	117.4 ± 14.8	–	–	–	–	–	–	0.2 ± 1.0	6.1	0.4 ± 3.2	3.2	0.2 ± 2.1	3.3
P. urnula	55.4 ± 2.0	75.3 ± 5.4	7.2 ± 12.6	82.0	1.1 ± 1.6	56.8	6.2 ± 9.6	81.8	3.8 ± 5.9	73.5	1.8 ± 2.7	51.6	3.4 ± 7.1	64.1
Salpingella acuminata	40.9 ± 2.7	268.7 ± 28.3	0.6 ± 1.3	26.0	0.2 ± 0.4	13.6	0.4 ± 0.8	24.2	–	–	0.0 ± 0.1	1.6	0.2 ± 0.6	9.6
S. faurei	13.8 ± 1.1	108.2 ± 6.1	2.8 ± 5.3	48.0	0.4 ± 0.8	22.7	0.6 ± 1.3	30.3	0.0 ± 0.1	2.0	0.1 ± 0.4	9.7	0.7 ± 2.4	18.9
Salpingella sp.1	12.1 ± 1.3	58.3 ± 7.7	22.3 ± 51.9	72.0	0.1 ± 0.3	9.1	4.1 ± 8.8	54.5	0.1 ± 0.4	10.2	0.0 ± 0.2	2.4	4.2 ± 22.7	21.9
Salpingella sp.2	14.1 ± 1.6	96.1 ± 10.8	0.2 ± 0.7	10.0	0.0 ± 0.2	2.2	0.0 ± 0.2	3.0	–	–	0.0 ± 0.2	2.4	0.0 ± 0.3	3.3
Neritic species														
Leprotintinnus pellucidus	38.5 ± 3.6	166.3 ± 38.9	–	–	–	–	–	–	0.1 ± 0.2	6.1	0.0 ± 0.1	0.8	0.0 ± 0.1	1.7
Stenosemella nivalis	24.1 ± 2.1	32.5 ± 2.1	–	–	–	–	–	–	–	–	0.1 ± 0.5	3.2	0.0 ± 0.3	1.3
*S. ventricosa**	35.9 ± 3.6	78.4 ± 3.1	–	–	–	–	–	–	–	–	0.0 ± 0.2	1.6	0.0 ± 0.1	0.7
*Tintinnopsis acuminata**	24.3	66.9	–	–	0.0 ± 0.2	2.2	–	–	–	–	–	–	0.0 ± 0.1	0.3
*T. beroidea**	18.2	55.2	–	–	0.0 ± 0.2	2.2	–	–	–	–	–	–	0.0 ± 0.1	0.3
*T. brasiliensis**	36.6	60.9	–	–	0.0 ± 0.2	2.2	–	–	–	–	–	–	0.0 ± 0.1	0.3
*T. lohmanni**	44.0 ± 4.7	75.0 ± 16.8	–	–	–	–	–	–	–	–	0.0 ± 0.2	0.8	0.0 ± 0.1	0.3
*T. parva**	26.5	49	–	–	–	–	–	–	–	–	0.0 ± 0.1	0.8	0.0 ± 0.1	0.3
T. rapa	25.3 ± 2.6	63.9 ± 5.9	–	–	–	–	–	–	0.0 ± 0.3	2.0	0.0 ± 0.3	2.4	0.0 ± 0.2	1.7
T. sinuata	44.0 ± 1.3	114.3 ± 13.5	–	–	–	–	–	–	–	–	0.1 ± 0.4	3.2	0.0 ± 0.3	1.7
*T. tubulosoides**	30.8 ± 3.7	81.7 ± 1.5	–	–	–	–	–	–	–	–	0.0 ± 0.2	0.8	0.0 ± 0.1	0.3
*T. urnula**	27.3	65.8	–	–	–	–	–	–	–	–	0.0 ± 0.3	0.8	0.0 ± 0.2	0.3

Species in red were regarded as abundant species with AA ≥ 3.0 ind. L^{-1} and OF ≥ 20%.
Abbreviations: LOD, lorica oral diameter (μm); LL, lorica length (μm); PSW, Pacific Summer Water; PWW, Pacific Winter Water; RWW, Remnant Winter Water; MLW, Mixed Layer Water; AtW, Atlantic-origin Water.
**species with counting number (n) < 10.*

increased to St. R7. As well as transect E, tintinnid abundance was highest in St. P1-2, then decreased northward through 20–50 m depths. High abundance areas along transects R and E occurred in the PSW and RWW, respectively (**Figures 2**, **3**).

Distribution of Abundant Tintinnid

Vertical distribution of different abundant species showed significant variations in different water masses. *Salpingella* sp.1 mainly occurred in layers between 25 and 75 m in the eastern part of transects P1, P2, and P3 (**Figure 3**). This species was not found in layers deeper than 100 m (**Figure 3**). High abundance (≥30 ind. L^{-1}) distribution area of *Salpingella* sp.1 was overlapped with the PSW (**Figures 2**, **3**).

High abundance (≥30 ind. L^{-1}) of *A. norvegica* occurred in ten stations at the western part of transects P1, P2, and P3 located at 25–50 m layers in most stations except St. P1-2, where abundance at surface layer reaches 174 ind. L^{-1} (**Figure 3**). The high abundance distribution area of *A. norvegica* overlapped with the RWW (**Figures 2**, **3**). We tracked stations with an abundance of *A. norvegica* higher than 100 ind. L^{-1}, and found that abundance decreased northward (**Figure 5**), which was the same for the direction of the Transpolar Drift (**Figures 1**, **5**).

Ptychocylis urnula occurred at all depths but mainly appeared in surface and DCM layers (**Figure 3**). In transects P1, P2, and P3, high abundance areas occurred in different depths in the western and eastern parts (**Figure 3**). In the eastern part, this species had a high abundance in surface waters, while in the western, its high abundance appears in the DCM layer (**Figure 3**).

Average Abundance, Occurrence Frequency, and Abundance Proportion of Abundant Tintinnids in Different Water Masses

The total abundance proportion of three abundant species (*Salpingella* sp. 1, *A. norvegica,* and *P. urnula*) was dominant (≥65.9%) in each water mass. In the PSW, RWW, and MLW, they occupied more than 89.7% (**Figure 4**). Tintinnid communities in different water masses had various diversity indices, with AtW (H' = 1.75, λ = 0.26) and RWW (H' = 0.54,

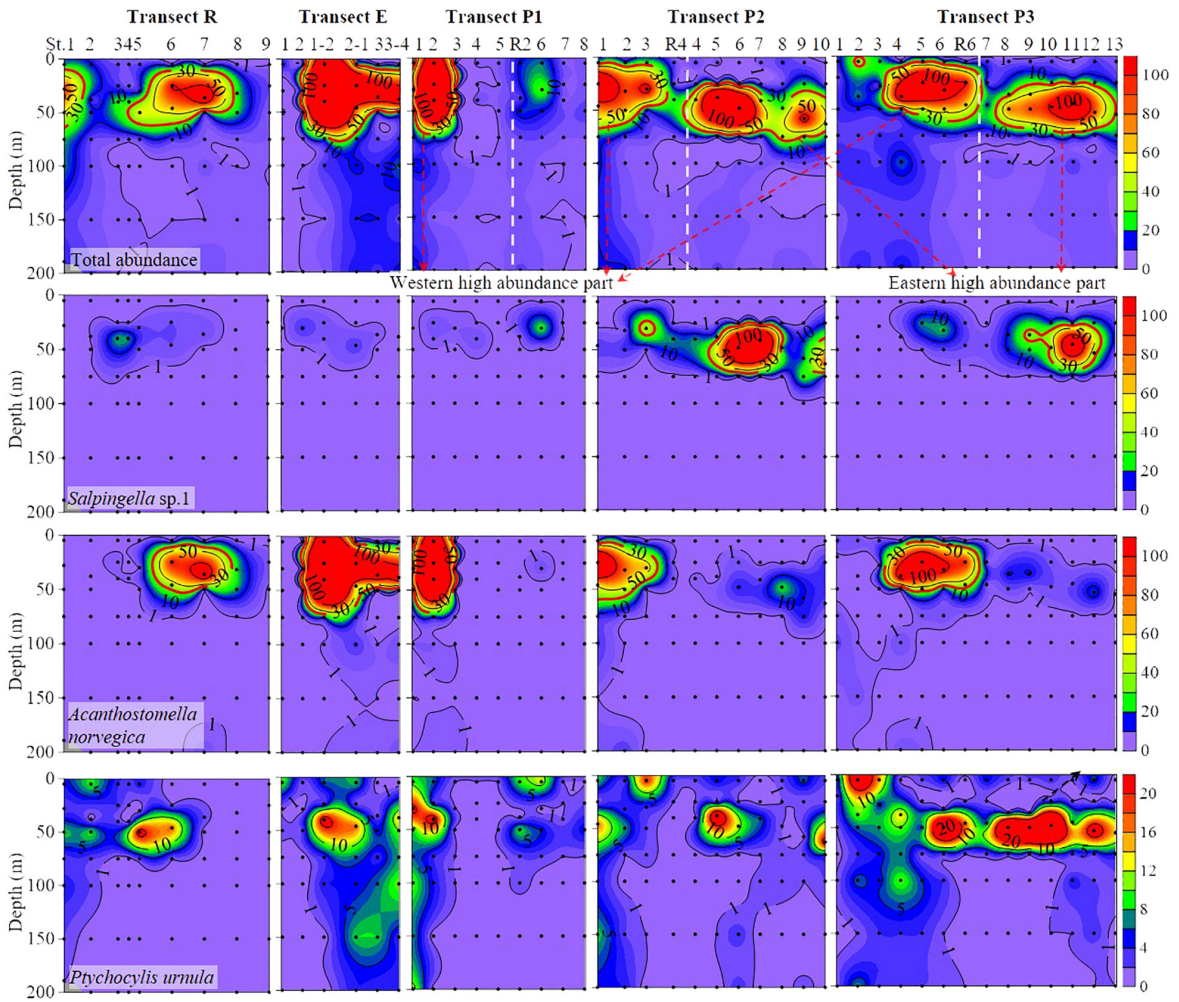

FIGURE 3 | Vertical distribution of total and abundant tintinnid abundance (ind. L^{-1}) from surface to 200 m. Black dots, sampling points. White dashed line, the boundary of western and eastern high abundance (≥30 ind. L^{-1}) part in transects P1, P2, and P3.

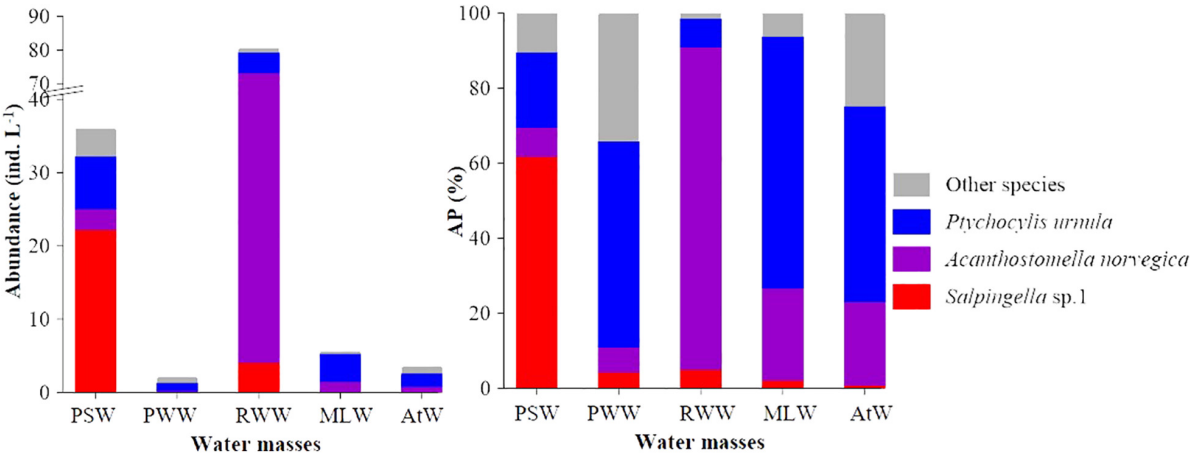

FIGURE 4 | Average abundance and abundance proportion (AP) of abundant tintinnids in different water masses. PSW, Pacific Summer Water; PWW, Pacific Winter Water; RWW, Remnant Winter Water; MLW, Mixed Layer Water; AtW, Atlantic-origin Water.

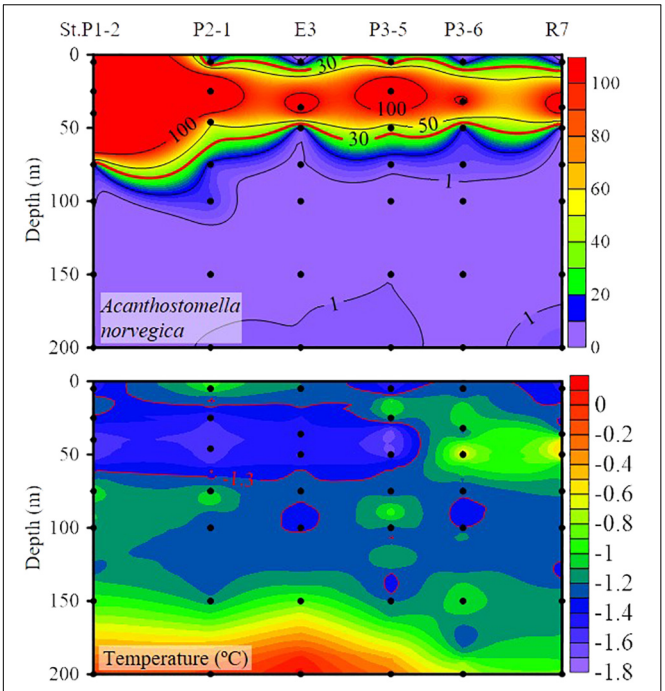

FIGURE 5 | Vertical distribution of *Acanthostomella norvegica* abundance (ind. L^{-1}) and temperature along the stations with *A. norvegica* maximum abundance higher than 100 ind. L^{-1}.

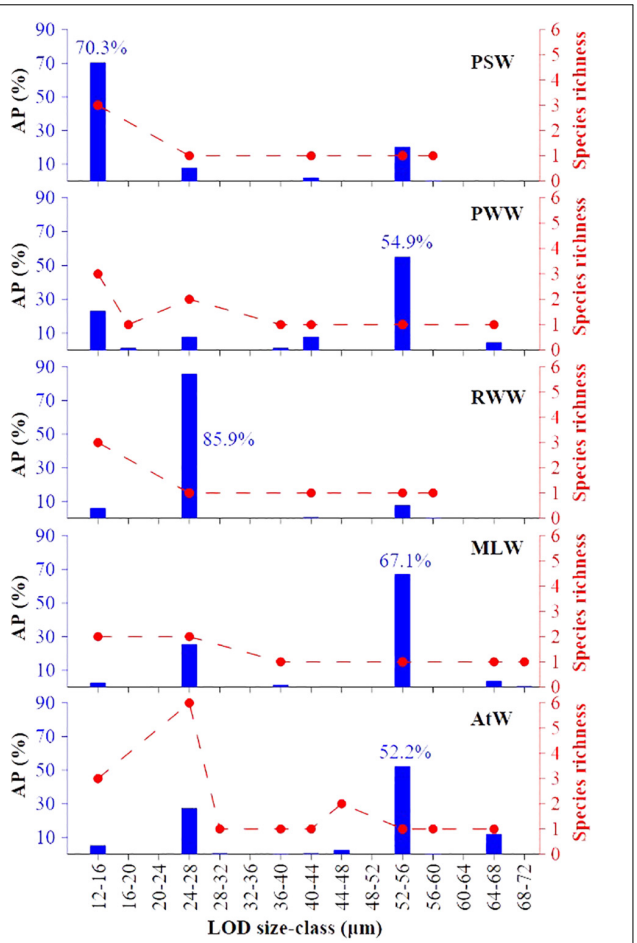

FIGURE 6 | Abundance proportion (AP) and species richness of tintinnid LOD (lorica oral diameter) size classes in each water mass. PSW, Pacific Summer Water; PWW, Pacific Winter Water; RWW, Remnant Winter Water; MLW, Mixed Layer Water; AtW, Atlantic-origin Water.

λ = 0.75) had highest and lowest tintinnid diversity, respectively (**Supplementary Table 2**).

In the PSW, *Salpingella* sp.1 and *P. urnula* were abundant species (**Table 2**). *Salpingella* sp.1 (AA = 22.3 ± 51.9 ind. L^{-1}, OF = 72.0%) had the highest average abundance, which was 3.1 and 8.0-folds of *P. urnula* (AA = 7.2 ± 12.6 ind. L^{-1}) and *A. norvegica* (AA = 2.8 ± 4.6 ind. L^{-1}), respectively (**Figure 4**). In addition, *Salpingella* sp.1 had highest abundance proportion (61.8%) among all the species. *P. urnula* (20.1%) and *A. norvegica* (7.8%) followed in sequence (**Figure 4**). The abundance proportion of other species was 10.3% (**Figure 4**). *P. urnula* (OF = 82.0%) had the highest occurrence frequency (**Table 2**).

In the RWW, *A. norvegica*, *P. urnula*, and *Salpingella* sp.1 were abundant species (**Table 2**). Among them, *A. norvegica* (AA = 69.2 ± 99.9 ind. L^{-1}, OF = 66.7%) had the highest average abundance, which was 11.2 and 16.9-folds of *P. urnula* (AA = 6.2 ± 9.4 ind. L^{-1}) and *Salpingella* sp.1 (4.1 ± 8.8 ind. L^{-1}), respectively (**Figure 4**). In addition, *A. norvegica* had the highest abundance proportion (85.9%) among all species. *P. urnula* (7.7%) and *Salpingella* sp.1 (5.1%) followed in sequence (**Figure 4**). The abundance proportion of other species was 1.4% (**Figure 4**). *P. urnula* (OF = 81.8%) had the highest occurrence frequency (**Table 2**).

In the MLW, PWW, and AtW, *P. urnula* had the highest average abundance (3.8 ± 5.9, 1.1 ± 1.6, and 1.8 ± 2.7 ind. L^{-1}, respectively) and occurrence frequency (73.5, 56.8, and 51.6%, respectively) (**Table 2**). In the MLW, this species was the sole abundant species. There were no abundant species in the PWW and AtW (**Table 2**). *A. norvegica* had second highest average abundance and occurrence frequency in the MLW (1.4 ± 3.4 ind. L^{-1}, OF = 32.7%) and AtW (0.8 ± 1.5 ind. L^{-1}, OF = 36.3%). The average abundance of *Salpingella* sp.1 was less than 0.1 ind. L^{-1} in these three water masses (**Figure 4** and **Table 2**). In the MLW, PWW, and AtW, *P. urnula* had highest abundance proportion (67.1, 54.9, and 52.2%, respectively) (**Figure 4**). *A. norvegica* had the second highest abundance proportion (24.5 and 22.2%) in the MLW and AtW. The abundance proportion of *Salpingella* sp.1 was less than 5.0% in these three water masses (**Figure 4**).

Abundance Proportion and Species Richness in Tintinnid Lorica Oral Diameter Size-Class

The abundance proportion of tintinnid LOD size classes in each water mass showed three distinctive tintinnid groups (**Figure 6**). The 12–16, 24–28, and 52–56 μm LOD size classes had the topmost value in the PSW (70.3%), RWW (85.9%), and other three water masses, respectively (**Figure 6**). Among them,

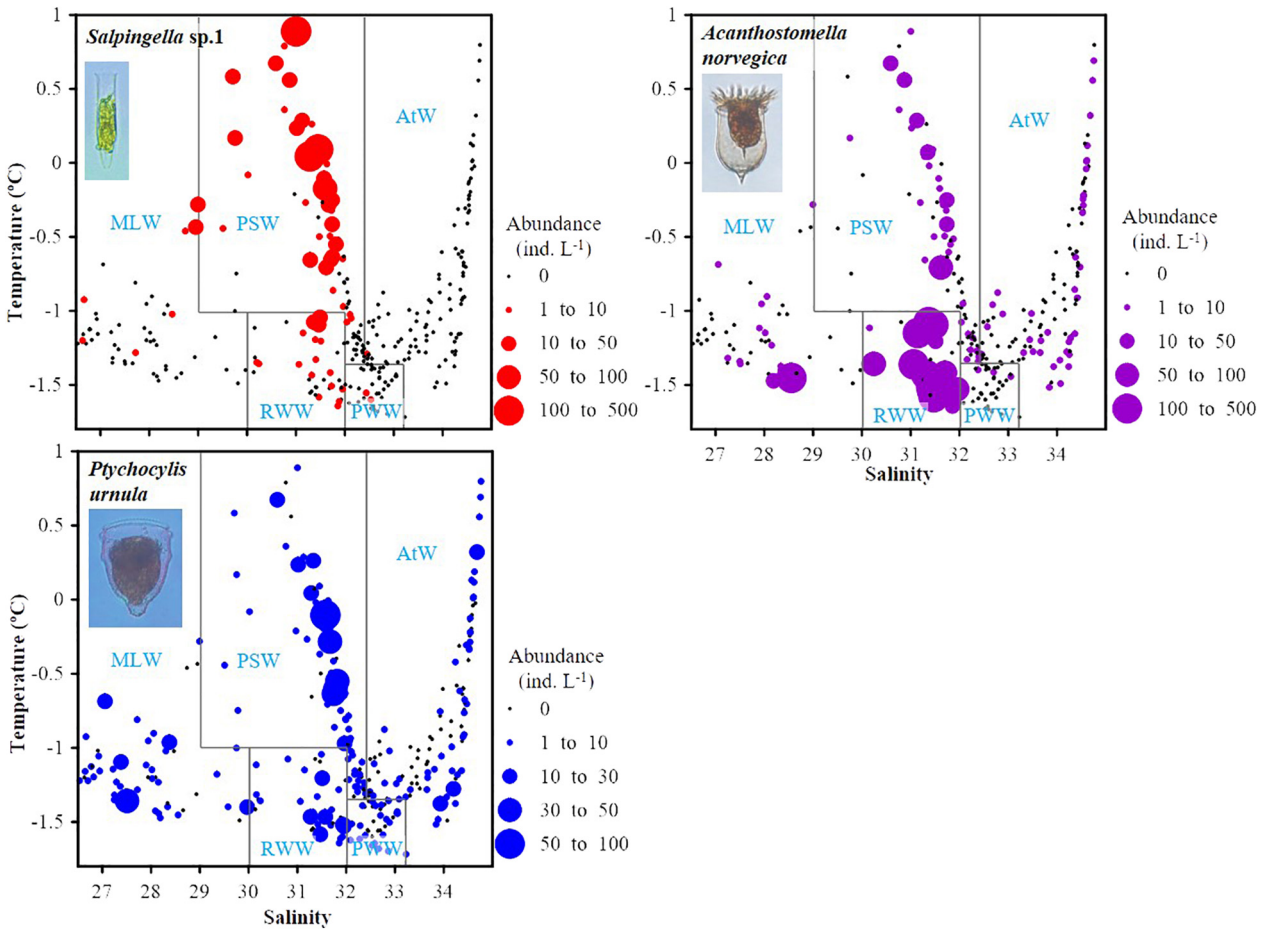

FIGURE 7 | Temperature-salinity-plankton diagrams for three abundant tintinnids in all water mass. Black dots represent sampling points where no species occurred. PSW, Pacific Summer Water; PWW, Pacific Winter Water; RWW, Remnant Winter Water; MLW, Mixed Layer Water; AtW, Atlantic-origin Water.

Salpingella sp.1 contributed most (81.9%) to the 12–16 μm LOD size-class in the PSW, and *A. norvegica* contributed most (100%) to the 24–28 μm LOD size-class in the RWW. *P. urnula* was the sole species in 52–56 μm LOD size-class. Its abundance proportion were highest in the MLW (67.1%), PWW (54.9%), and AtW (52.2%) (**Figure 6**). High abundance proportion and the number of species richness in tintinnid LOD (lorica oral diameter) size classes were not consistent in the PWW and AtW. Although the number of species richness in 12–16 and 24–28 μm LOD size-classes were highest in the PWW and AtW, the highest abundance proportion were both 52–56 μm LOD size-classes (**Figure 6**).

Relationship Between Abundant Tintinnids and Environmental Factors

Temperature-salinity-plankton diagrams showed that the three abundant species had different temperature and salinity ranges. High abundance (≥30 ind. L^{-1}) of *Salpingella* sp.1 mainly distributed in relatively higher temperature (−1.0–0.9°C) but narrower salinity range (31.0–32.0) than *A. norvegica* (−1.7– -1.0°C, 28.5–32.0) (**Figure 7**). *P. urnula* had the widest temperature (−1.7–0.9°C) and salinity (26.6–34.7) range (**Figure 7**).

Each abundant tintinnid had a different correlation with environmental factors (depth, temperature, salinity, and Chl *a*) (**Table 3**). Three abundant tintinnids had a significant negative correlation with depth. *A. norvegica* and *Salpingella* sp.1 had a positive correlation with temperature. *P. urnula* and *Salpingella* sp.1 had a significant negative correlation with salinity. All abundant tintinnid abundance had less correlation with Chl *a* (**Table 3**). The significant positive correlation between *Salpingella*

TABLE 3 | Spearman's rank correlation between the abundant tintinnid abundance (ind. L^{-1}) and depth (m), temperature (°C), salinity, and the Chl *a* (μg L^{-1}).

Species	Depth	Temperature	Salinity	Chl *a*
Acanthostomella norvegica	−0.199**	0.138*	−0.108	0.004
Ptychocylis urnula	−0.270**	0.038	−0.163**	−0.061
Salpingella sp.1	−0.346**	0.285**	−0.335**	0.098

***: $p < 0.01$, *: $p < 0.05$, t-test.*

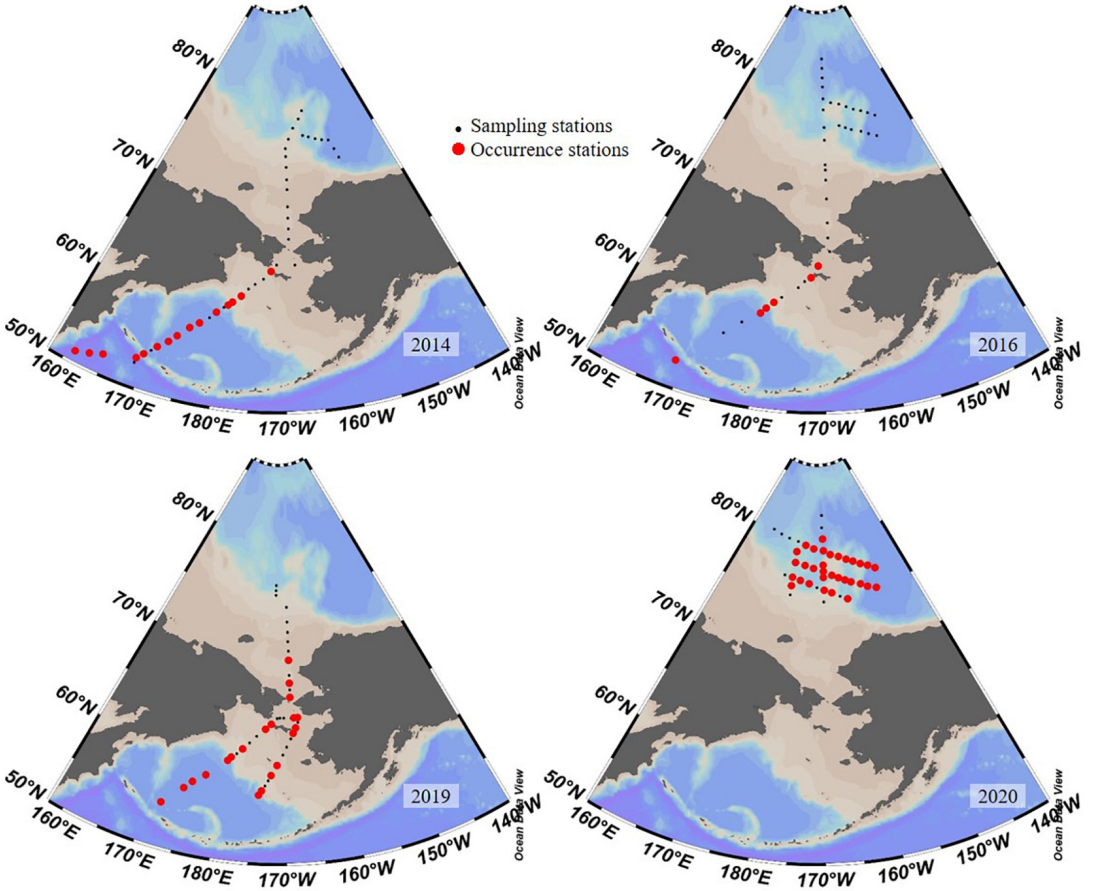

FIGURE 8 | Existence of *Salpingella* sp.1 in years 2014 (Li et al., 2016), 2016 (Wang et al., 2019), 2019 (our unpublished data), and 2020.

sp.1 and temperature determined that this species is mainly distributed in the PSW of the Canada Basin (**Figure 8**).

DISCUSSION

Tintinnid Community Structure Variations in Different Water Masses

Tintinnid community structure variations in different water masses are scarcely studied in the Arctic basin. Our result showed that *Salpingella* sp.1 had a high abundance in the PSW of the Canada Basin. The entire vertical structure shape of the PSW in the Canada Basin was like a bowl that was distributed between the Arctic MLW and PWW (Steele et al., 2004; Bluhm et al., 2015; Manucharyan and Spall, 2016). Although our sampling transects only occupied part of the PSW. By examining the combined high abundance of *Salpingella* sp.1 and bowl-like structure of the PSW connectivity, we speculate that species *Salpingella* sp.1 could be distributed across the whole PSW of the Canada Basin. The obvious high abundance of *Salpingella* sp.1 in the PSW was the reason for lower tintinnid diversity in this water mass than in PWW.

Acanthostomella norvegica was a dominant species in the Bering Sea (Taniguchi, 1984; Dolan et al., 2014; Li et al., 2016; Wang et al., 2019). Previous studies have reported *A. norvegica* with low abundance in the Arctic Ocean, with an average abundance $\leq$0.8 ind. L^{-1} in Dolan et al. (2014) and A_{max} = 5 ind. L^{-1} in Wang et al. (2019). However, there was no information about its origin. Our results showed an extremely low abundance of *A. norvegica* in stations Sts. E1, E2, P1-4, R1, P3-8 (**Figure 3**), which are located in pathways of Pacific Inflow Water (Steele et al., 2004; Aksenov et al., 2016; Hunt et al., 2016; Li et al., 2019; Zhong et al., 2019). Therefore, we concluded that the high abundance of *A. norvegica* in the RWW did not originate from the Bering Sea. On the other hand, *A. norvegica* had the highest abundance among all tintinnid species in the Barents Sea (Boltovskoy et al., 1991; Monti and Minocci, 2013), where the main stream of the Atlantic Inflow Water flows over (Aksenov et al., 2016). Comparing the trajectories of the Atlantic Inflow Water along the slope and the *A. norvegica* abundance northward decrease trend in the RWW (**Figure 4**), we speculated that this species might originate from the North Atlantic and merge into the main stream of the Transpolar Drift (Steele et al., 2004; Johannessen et al., 2012). In addition, transect R was the boundary separating the high abundance stations of *Salpingella*

sp. 1 and *A. norvegica* in this study (**Figure 1**). The spatial division of *Salpingella* sp. 1 and *A. norvegica* might manifest the interaction between the Beaufort Gyre and Transpolar Drift.

The LOD of a tintinnid is related to its preferred food item size [about 25% of the LOD (Dolan, 2010)]. Previous studies have shown that larger LOD (LOD > 40 μm) comprised >60% in the Arctic Ocean in 2011 (63.3%, Dolan et al., 2014) and 2016 (89.1%, Wang et al., 2019). Our results showed that abundance proportions of 12–16 μm LOD size-class were dominant, which was different from the previous study that indicated that a larger (60–64 μm) LOD size-class was dominant in the PSW of the Canada Basin (Wang C. F. et al., 2020). Thus, the tintinnid community size is smaller in the Canada Basin in the 2020 cruise. This phenomenon revealed that the preferred food item size for tintinnid had changed from 15–16 to 3–4 μm, which was consistent with the decreasing trend of phytoplankton size classes (Li et al., 2009; Zhuang et al., 2021).

Transport of Pacific Species Into the Canada Basin

Ptychocylis urnula was the dominant species (Dolan et al., 2014; Wang et al., 2019) and there was no *Salpingella* sp.1 in the western Arctic Ocean in August 2016 (Wang et al., 2019). Our results revealed that dominant species in the PSW of the Canada Basin changed to *Salpingella* sp.1 with a much higher abundance than *P. urnula*. *Salpingella* sp.1 was first recorded in surface waters of the northwest Pacific in the summer of 2014 (Li et al., 2016). Its abundance decreased from northwest Pacific (A_{max} = 34.5 ind. L^{-1}) to the Bering Sea (<10 ind. L^{-1}) and eventually disappeared near the Bering Strait (Li et al., 2016). In 2016, a low abundance (A_{max} = 12 ind. L^{-1}) of this species was reported in the Bering Sea (Wang et al., 2019). Our unpublished data in summer 2019 also found that this species had a higher abundance (A_{max} = 517 ind. L^{-1}) in the northern Bering Sea. But this species was not found in adjacent areas of the Canada Basin during summer 2014 (Li et al., 2016) and 2016 (Wang et al., 2019; **Figure 8**). Therefore, we concluded that this species in the PSW in summer 2020 originated from the North Pacific.

Due to its having higher salinity than Arctic surface water, the Pacific Inflow Water sank into subsurface layers of the Canada Basin and became PSW (Carmack et al., 2016; Zhong et al., 2019; Polyakov et al., 2020), causing the mixing between the Arctic and Pacific zooplankton. Previous studies have reported that mesozooplankton copepods species (*M. pacifica*, *Neocalanus cristatus*, *N. plumchrus,* and *E. bungii*) from the Bering Sea were found in the Canada Basin (Ershova et al., 2015; Wassmann et al., 2015; Kim et al., 2020). Because these samples were obtained by net towing from the bottom (or 200 m) to the surface, it is hard to confirm the exact layers of copepod species in the PSW. The Pacific copepod species found in the Canada Basin might be transported by surface eddies from the Alaska shelf break (Watanabe, 2011; Watanabe et al., 2012). Our samples were obtained by CTD at exact layers. Therefore, our result (*Salpingella* sp. 1 in the PSW of the Arctic Ocean) is the first to confirm the occurrence of Pacific plankton in the PSW of the Canada Basin.

The position of our stations in eastern parts of transects P2 (Sts. 5–10) and P3 (Sts. 7–13) were similar to stations in transects P2 (Sts. 22–27) and P1 (Sts. 11–17) of 2016, respectively (Wang et al., 2019). The survey time in Wang et al. (2019) (from 28 July to 3 August 2016) was also similar to our sampling time (from 6 to 11 August 2020). In the Beaufort Gyre of the Canada Basin, the PSW was characterized by a temperature higher than −1°C (Steele et al., 2004). After comparing the thickness of the PSW between 2016 (Wang et al., 2019) and our data the surface to a 200 m depth (every 1 m had one temperature value), we found that the transects P2 (average 85.3 ± 13.5 m) and P3 (average 75.9 ± 25.3 m) in the eastern parts of 2020 were 12.8 and 4.1 m thicker than transects P2 (average 72.5 ± 19.3 m) and P1 (average 71.7 ± 18.7 m) of 2016 (Wang et al., 2019). The maximum temperature of the PSW in 2020 (1.1°C) was similar to 2016 (1.0°C), but the average temperature of 2020 in eastern parts of transects P2 (average −0.2 ± 0.5°C) and P3 (average −0.2 ± 0.6°C) were 0.5 and 0.1°C higher than P2 (average −0.7 ± 0.3°C) and P1 (average −0.3 ± 0.6°C) of 2016, respectively. Because *Salpingella* sp.1 had a significant positive correlation with temperature, we speculated that the increase in PSW thickness and average temperature might account for the high abundance of *Salpingella* sp.1 in the PSW in the year 2020.

The percentage of empty lorica of *Salpingella* sp.1 was 1.3%. Therefore, we speculated that most of *Salpingella* sp.1 were alive during sampling time. In this study, a high abundance of *Salpingella* sp.1 occurred in PSW with a water temperature range from −0.3 to 0.9°C. This species might have a strong adaptation and reproduce to establish a local population in the PSW, or might be in functionally sterile expatriate status (Wassmann et al., 2015) in low temperature conditions. Our results only present a "snapshot" phenomenon in summer 2020. We do not know whether this phenomenon occurred before and how long this species will persist throughout the year. Further investigations in the North Pacific and Canada Basin are needed to answer these questions.

CONCLUSION

The present study reported on tintinnid species richness, vertical distribution, and relationship with environmental factors in different water masses in the Arctic Ocean in summer 2020. Five water masses were identified and each of them had a distinct tintinnid community structure, which confirms our hypothesis. In the PSW, *Salpingella* sp.1 was an abundant species and had the highest abundance proportion. In the RWW, *A. norvegica* was an abundant species and had the highest abundance proportion. *Salpingella* sp.1, which originated from the north Pacific, occupied a much higher abundance proportion than previous Arctic dominant species, *Ptychocylis urnula* in the PSW.

DATA AVAILABILITY STATEMENT

The original contributions presented in the study are included in the article/**Supplementary Material**, further inquiries can be directed to the corresponding authors.

AUTHOR CONTRIBUTIONS

CW and XW: field sampling, tintinnid taxonomy, counting, data analysis, and writing-original draft. ZX and QH: field sampling and data analysis. YZ, WZ, and TX: conceptualization and writing-original draft. All authors contributed to the article and approved the submitted version.

FUNDING

This research was funded by the China Postdoctoral Science Foundation (grant number 2020M672149), the National Key Research and Development Program of China (grant number 2019YFA0607001), the Applied Research Project for Postdoctoral in Qingdao, and the National Natural Science Foundation of China (grant numbers 41706217 and 42076225).

ACKNOWLEDGMENTS

Special thanks to the captain and crews of R.V. "Xuelong 2" for their great help in sampling during the 11th Chinese National Arctic Research Expedition. We thank Steve O'Shea, from Edanz (https://jp.edanz.com), for editing a draft of this manuscript. We greatly appreciate the constructive comments by the three reviewers, which improved the quality of the manuscript.

SUPPLEMENTARY MATERIAL

The Supplementary Material for this article can be found online at: https://www.frontiersin.org/articles/10.3389/fmars.2021.775653/full#supplementary-material

REFERENCES

Aksenov, Y., Ivanov, V. V., Nurser, A. J. G., Bacon, S., Polyakov, I. V., Coward, A. C., et al. (2011). The Arctic circumpolar boundary current. *J. Geophys. Res.* 116:C09017. doi: 10.1029/2010JC006637

Aksenov, Y., Karcher, M., Proshutinsky, A., Gerdes, R., Cuevas, B., Golubeva, E., et al. (2016). Arctic pathways of Pacific Water: Arctic ocean model intercomparison experiments. *J. Geophys. Res. Oceans* 121, 27–59. doi: 10.1002/2015JC011299

Alder, V. A. (1999). "Tintinnoinea," in *South Atlantic Zooplankton*, ed. D. Boltovskoy (Leiden: Backhuys), 321–384.

Azam, F., Fenchel, T., Field, J. G., Gray, J. S., Meyer-Reil, L. A., and Thingstad, F. (1983). The ecological role of water column microbes in the sea. *Mar. Ecol. Prog. Ser.* 10, 257–263. doi: 10.3354/meps010257

Bluhm, B. A., Kosobokova, K. N., and Carmack, E. C. (2015). A tale of two basins: an integrated physical and biological perspective of the deep Arctic Ocean. *Prog. Oceanogr.* 139, 89–121. doi: 10.1016/j.pocean.2015.07.011

Boltovskoy, D., Vivequin, S. M., and Swanberg, N. R. (1991). Vertical distribution of tintinnids and associated microplankton in the upper layer of the Barents Sea. *Sarsia* 76, 141–151. doi: 10.1080/00364827.1991.10413469

Calbet, A., and Saiz, E. (2005). The ciliate-copepod link in marine ecosystems. *Aquat. Microb. Ecol.* 38, 157–167. doi: 10.3354/ame038157

Carmack, E. C., Yamamoto-Kawai, M., Haine, T., Bacon, S., Bluhm, B. A., Lique, C., et al. (2016). Freshwater and its role in the Arctic Marine ecosystem: sources, disposition, storage, export, and physical and biogeochemical consequences in the Arctic and global oceans. *J. Geophys. Res. Biogeosci.* 121, 675–717. doi: 10.1002/2015JG003140

Davis, C. C. (1977). Variations of the lorica in the genus *Parafavella* (Protozoa: Tintinnida) in northern Norway waters. *Can. J. Zool.* 56, 1822–1827. doi: 10.1139/z78-248

Davis, C. C. (1981). Variations of lorica shape in the genus *Ptychocylis* (Protozoa: Tintinnina) in relation to species identification. *J. Plankton Res.* 3, 433–443. doi: 10.1093/plankt/3.3.433

Dolan, J. R. (2010). Morphology and ecology in tintinnid ciliates of the marine plankton: correlates of lorica dimensions. *Acta Protozoologica* 49, 235–244.

Dolan, J. R., and Pierce, R. W. (2013). "Diversity and distributions of tintinnid ciliates," in *The Biology and Ecology of Tintinnid Ciliates: Models for Marine Plankton*, eds J. R. Dolan, S. Agatha, and D. W. Coats (Oxford: Wiley-Blackwell), 214–243. doi: 10.1002/9781118358092.ch10

Dolan, J. R., Pierce, R. W., and Yang, E. J. (2017). Tintinnid ciliates of the marine microzooplankton in Arctic Seas: a compilation and analysis of species records. *Polar Biol.* 40, 1247–1260. doi: 10.1007/s00300-016-2049-0

Dolan, J. R., Vidussi, F., and Claustre, H. (1999). Planktonic ciliates in the Mediterranean Sea: longitudinal trends. *Deep Sea Res. Part I Oceanogr. Res. Pap.* 46, 2025–2039. doi: 10.1016/S0967-0637(99)00043-6

Dolan, J. R., Yang, E. J., Kang, S. H., and Rhee, T. S. (2016). Declines in both redundant and trace species characterize the latitudinal diversity gradient in tintinnid ciliates. *ISME J.* 10, 2174–2183. doi: 10.1038/ismej.2016.19

Dolan, J. R., Yang, E. J., Kim, T. W., and Kang, S. H. (2014). Microzooplankton in warming Arctic: a comparison of tintinnids and radiolarians from summer 2011 and 2012 in the Chukchi Sea. *Acta Protozool.* 52, 101–113.

Ershova, E. A., Hopcroft, R. R., Kosobokova, K. N., Matsuno, K., Nelson, R. J., Yamaguchi, A., et al. (2015). Long-term changes in summer zooplankton communities of the western Chukchi Sea, 1945-2012. *Oceanography* 28, 100–115. doi: 10.5670/oceanog.2015.60

Gerdes, R., and Schauer, U. (1997). Large-scale circulation and water mass distribution in the Arctic Ocean from model results and observations. *J. Geophys. Res. Oceans* 102, 8467–8483. doi: 10.1029/97JC00102

Gómez, F. (2007). Trends on the distribution of ciliates in the open Pacific Ocean. *Acta Oecol.* 32, 188–202. doi: 10.1016/j.actao.2007.04.002

Gong, D., and Pickart, R. S. (2016). Early summer water mass transformation in the eastern Chukchi Sea. *Deep Sea Res. II.* 130, 43–55. doi: 10.1016/j.dsr2.2016.04.015

Grebmeier, J. M., and Harvey, H. R. (2005). The Western Arctic Shelf-Basin Interactions (SBI) project: an overview. *Deep Sea Res. II.* 52, 3109–3576. doi: 10.1016/j.dsr2.2005.10.004

Hopcroft, R. R., Kosobokova, K. N., and Pinchuk, A. I. (2010). Zooplankton community patterns in the Chukchi Sea during summer 2004. *Deep Sea Res. II.* 57, 27–39. doi: 10.1016/j.dsr2.2009.08.003

Hunt, G. L., Drinkwater, K. F., Arrigo, K., Berge, J., Daly, K. L., Danielson, S., et al. (2016). Advection in polar and sub-polar environments: impacts on high latitude marine ecosystems. *Prog. Oceanogr.* 149, 40–81. doi: 10.1016/j.pocean.2016.10.004

Johannessen, O. M., Miles, M. W., Bengtsson, L., Bobylev, L. P., and Kuzmina, S. I. (2012). *Arctic Climate Change*. Dordrecht: Springer, 1–146.

Kato, S., and Taniguchi, A. (1993). Tintinnid ciliates as indicator species of different water masses in the western North Pacific Polar Front. *Fish. Oceanogr.* 2, 166–174. doi: 10.1111/j.1365-2419.1993.tb00132.x

Kim, J. H., Cho, K. H., La, H. S., Choy, E. J., and Yang, E. J. (2020). Mass occurrence of Pacific copepods in the southern Chukchi Sea during summer: implications of the high-temperature Bering Summer Water. *Front. Mar. Sci.* 7:612. doi: 10.3389/fmars.2020.00612

Knap, A. H., Michaels, A., Close, A. R., Ducklow, H., and Dickson, A. G. (1996). Protocols for the joint global ocean flux study (JGOFS) core measurements. *JGOFS Rep.* 19, 155–162.

Lewis, K. M., Van Dijken, G. L., and Arrigo, K. R. (2020). Changes in phytoplankton concentration now drive increased Arctic Ocean primary production. *Science* 369, 198–202. doi: 10.1126/science.aay8380

Li, H. B., Xu, Z. Q., Zhang, W. C., Wang, S., Zhang, G. T., and Xiao, T. (2016). Boreal tintinnid assemblage in the Northwest Pacific and its connection with

the Japan Sea in summer 2014. *PLoS One* 11:e0153379. doi: 10.1371/journal.pone.0153379

Li, M., Pickart, R. S., Spall, M. A., Weingartner, T. J., Lin, P. G., Moore, G. W. K., et al. (2019). Circulation of the Chukchi Sea shelfbreak and slope from moored timeseries. *Prog. Oceanogr*. 172, 14–33. doi: 10.1016/j.pocean.2019.01.002

Li, W., Mclaughlin, F. A., Lovejoy, C., and Carmack, E. C. (2009). Smallest algae thrive as the Arctic Ocean freshens. *Science* 326, 539–539. doi: 10.1126/science.1179798

Liang, C., Li, H. B., Dong, Y., Zhao, Y., Tao, Z. C., Li, C. L., et al. (2018). Planktonic ciliates in different water masses in open waters near Prydz Bay (East Antarctica) during austral summer, with an emphasis on tintinnid assemblages. *Polar Biol.* 41, 2355–2371. doi: 10.1007/s00300-018-2375-5

Liang, C., Li, H. B., Zhang, W. C., Tao, Z. C., and Zhao, Y. (2019). Changes in tintinnid assemblages from subantarctic zone to Antarctic zone along transect in Amundsen Sea (west Antarctica) in early austral autumn. *J. Ocean Univ. China* 19, 339–350. doi: 10.1007/s11802-020-4129-6

Lund, J. W. G., Kipling, C., and Cren, E. D. L. (1958). The inverted microscope method of estimating algal numbers and the statistical basis of estimations by counting. *Hydrobiologia* 11, 143–170. doi: 10.1007/BF00007865

Lynn, D. H. (2008). *Ciliated Protozoa: Characterization, Classification, and Guide to the Literature*, 3rd Edn. Berlin: Springer, 1–455.

Mańko, M. K., Guchowska, M., and Agata, W. Z. (2020). Footprints of Atlantification in the vertical distribution and diversity of gelatinous zooplankton in the Fram Strait (Arctic Ocean). *Prog. Oceanogr.* 189:102414. doi: 10.1016/j.pocean.2020.102414

Manucharyan, G. E., and Spall, M. A. (2016). Wind-driven freshwater buildup and release in the Beaufort Gyre constrained by mesoscale eddies. *Geophys. Res. Lett.* 43, 273–282. doi: 10.1002/2015GL065957

McLaughlin, F. A., Carmack, E. C., Macdonald, R. W., Melling, H., Swift, J. H., Wheeler, P. A., et al. (2004). The joint roles of Pacific and Atlantic-origin waters in the Canada Basin, 1997-1998. *Deep Sea Res. Part I Oceanogr. Res. Pap.* 51, 107–128. doi: 10.1016/j.dsr.2003.09.010

Møller, E. F., and Nielsen, T. G. (2020). Borealization of Arctic zooplankton-smaller and less fat zooplankton species in Disko Bay. *Western Greenland. Limnol. Oceanogr.* 65, 1175–1188. doi: 10.1002/lno.11380

Monti, M., and Minocci, M. (2013). Microzooplankton along a transect from nothern continental Norway to Svalbard. *Polar Res.* 32:19306. doi: 10.3402/polar.v32i0.19306

Morison, J., Steele, M., and Andersen, R. (1998). Hydrography of the upper Arctic Ocean measured from the nuclear submarine U.S.S. Pargo. *Deep Sea Res. Part I Oceanogr. Res. Pap.* 45, 15–38. doi: 10.1016/S0967-0637(97)00025-3

Paranjape, M. A., and Gold, K. (1982). Cultivation of marine pelagic protozoa. *Ann. Inst. Oceanogr. Paris* 58, 143–150. doi: 10.1128/AEM.67.5.2145-2155.2001

Pierce, R. W., and Turner, J. T. (1992). Ecology of planktonic ciliates in marine food webs. *Rev. Aquat. Sci.* 6, 139–181.

Pierce, R. W., and Turner, J. T. (1993). Global biogeography of marine tintinnids. *Mar. Ecol. Prog. Ser.* 94, 11–26. doi: 10.3354/meps094011

Polyakov, I., Alkire, M. B., Bluhm, B. A., Brown, K. A., and Wassmann, P. (2020). Borealization of the Arctic Ocean in response to anomalous advection from sub-Arctic seas. *Front. Mar. Sci.* 7:491. doi: 10.3389/fmars.2020.00491

Rakshit, D., Sahu, G., Mohanty, A. K., Satpathy, K. K., Jonathan, M. P., Murugan, K., et al. (2017). Bioindicator role of tintinnid (Protozoa: Ciliophora) for water quality monitoring in Kalpakkam, Tamil Nadu, south east coast of India. *Mar. Pollut. Bull.* 114, 134–143. doi: 10.1016/j.marpolbul.2016.08.058

Shannon, C. E. (1948). A mathematical theory of communication. *Bell. System. Techn. J.* 27, 379–423. doi: 10.1002/j.1538-7305.1948.tb01338.x

Simpson, E. H. (1949). Measurement of diversity. *Nature* 163:688. doi: 10.1038/163688a0

Steele, M., Morison, J., Ermold, W., Rigor, I., and Ortmeyer, M. (2004). Circulation of summer Pacific halocline water in the Arctic Ocean. *J. Geophys. Res.* 109:C02027. doi: 10.1029/2003JC002009

Stoecker, D. K., Michaels, A. E., and Davis, L. H. (1987). Grazing by the jellyfish, *Aurelia aurita*, on microzooplankton. *J. Plankton Res.* 9, 901–915. doi: 10.1093/plankt/9.5.901

Taniguchi, A. (1976). Microzooplankton and seston in Akkeshi Bay, Japan. *Hydrobiologia* 50, 195–204. doi: 10.1007/BF00020992

Taniguchi, A. (1984). Microzooplankton biomass in Arctic and subarctic Pacific Ocean in summer. *Mem. Natl. Inst. Polar Res. Spec. Issue* 32, 63–80.

Timmermans, M. L., Proshutinsky, A., Golubeva, E., Jackson, J. M., Krishfield, R., McCall, M., et al. (2014). Mechanisms of Pacific Summer Water variability in the Arctic's Central Canada Basin. *J. Geophys. Res. Oceans* 119, 7523–7548. doi: 10.1002/2014JC010273

Trenberth, K. E., Jones, P. D., Ambenje, P., Bojariu, R., Easterling, D., Klein Tank, A., et al. (eds) (2007). "Observations: surface and atmospheric climate change: climate change 2007: the physical science basis," in *Contribution of Working Group I to the Fourth Assessment Report of the Intergovernmental Panel on Climate Change*, eds S. Solomon, D. Qin, M. Manning, Z. Chen, M. Marquis, K. B. Averyt, et al. (Cambridge: Cambridge University Press).

Utermöhl, H. (1958). Zur vervollkommnung der quantitativen phytoplankton Methodik. *Mit. Int. Ver. Theor. Angew. Limnol.* 9, 1–38. doi: 10.1080/05384680.1958.11904091

Wang, C. F., Li, H. B., Xu, Z. Q., Zheng, S., Hao, Q., Dong, Y., et al. (2020). Difference of planktonic ciliate communities of the tropical West Pacific, the Bering Sea and the Arctic Ocean. *Acta Oceanol. Sin.* 39, 9–17. doi: 10.1007/s13131-020-1541-0

Wang, C. F., Xu, Z. Q., Liu, C. G., Li, H. B., Liang, C., Zhao, Y., et al. (2019). Vertical distribution of oceanic tintinnid (Ciliophora: Tintinnida) assemblages from the Bering Sea to Arctic Ocean through Bering Strait. *Polar Biol.* 42, 2105–2117. doi: 10.1007/s00300-019-02585-2

Wang, Y., Kang, J., Xiang, P., Wang, W., and Lin, M. (2020). Short timeframe changes of environmental impacts on summer phytoplankton in the Chukchi Sea and surrounding areas in a regional scaling. *Ecol. Indic.* 117:106693. doi: 10.1016/j.ecolind.2020.106693

Wang, Y., Xiang, P., Kang, J. H., Ye, Y. Y., Lin, G. M., and Yang, Q. L. (2018). Environmental controls on spatial variability of summer phytoplankton structure and biomass in the Bering Sea. *J. Sea Res.* 131, 1–11. doi: 10.1016/j.seares.2017.08.008

Wassmann, P., Kosobokova, K. N., Slagstad, D., Drinkvvater, K. F., Hoperoft, R. R., Moore, S. E., et al. (2015). The contiguous domains of Arctic Ocean advection: trails of life and death. *Prog. Oceanogr.* 139, 42–65. doi: 10.1016/j.pocean.2015.06.011

Watanabe, E. (2011). Beaufort shelf break eddies and shelf-basin exchange of Pacific summer water in the western Arctic Ocean detected by satellite and modeling analyses. *J. Geophys. Res.* 116:C08034. doi: 10.1029/2010JC006259

Watanabe, E., Kishi, M. J., Ishida, A., and Aita, M. N. (2012). Western Arctic primary productivity regulated by shelf-break warm eddies. *J. Oceanogr.* 68, 703–718. doi: 10.1007/s10872-012-0128-6

Woodgate, R. A. (2018). Increasing in the Pacific inflow to the Arctic from 1990 to 2015, and insights into seasonal trends and driving mechanisms from year-round Bering Strait mooring data. *Prog. Oceanogr.* 160, 124–154. doi: 10.1016/j.pocean.2017.12.007

Zhang, W. C., Feng, M. P., Yu, Y., Zhang, C. X., and Xiao, T. (2012). *An Illustrated Guide to Contemporary Tintinnids in the World*. Beijing: Science Press, 1–499.

Zhong, W., Steele, M., Zhang, J., and Cole, S. T. (2019). Circulation of Pacific winter water in the Western Arctic Ocean. *J. Geophys. Res. Oceans* 124, 863–881. doi: 10.1029/2018JC014604

Zhuang, Y., Jin, H., Zhang, Y., Li, H., Zhang, T., Li, Y., et al. (2021). Incursion of Alaska coastal water as a mechanism promoting small phytoplankton in the western Arctic Ocean. *Prog. Oceanogr.* 197:102639. doi: 10.1016/j.pocean.2021.102639

Conflict of Interest: The authors declare that the research was conducted in the absence of any commercial or financial relationships that could be construed as a potential conflict of interest.

Publisher's Note: All claims expressed in this article are solely those of the authors and do not necessarily represent those of their affiliated organizations, or those of the publisher, the editors and the reviewers. Any product that may be evaluated in this article, or claim that may be made by its manufacturer, is not guaranteed or endorsed by the publisher.